THE ASTROPHYSICAL JOURNAL, 422:208–218, 1994 February 10

RELATIVISTIC PRECESSION OF THE ORBIT OF A STAR NEAR A SUPERMASSIVE BLACK HOLE

V. KARAS[1,2] AND D. VOKROUHLICKÝ[1]
Received 1993 February 9; accepted 1993 April 26

ABSTRACT

We study the gravitomagnetic (Lense-Thirring) precession of the trajectory (approximated by a geodesic) of a star orbiting supermassive rotating (Kerr) black hole. We do not assume any particular value for the eccentricity or inclination of the orbit or the angular momentum of the black hole. We also discuss the periodicity related to the relativistic shift of the pericenter.

Subject headings: black hole physics — galaxies: active — relativity

1. INTRODUCTION

It is widely accepted that supermassive black holes (SBHs) are located in cores of active galaxies and quasars (Begelman, Blandford, & Rees 1984; Shlosman, Begelman, & Frank 1990). The mass of the SBH is usually estimated to be in the range $M \approx 10^6$–$10^{11}\ M_\odot$. Anomalous energy output of active galactic nuclei (AGNs) may result from an accretion process: the matter is attracted from the surroundings of an AGN, or it comes from tidally disrupted stars passing too close to the SBH. The accretion disk is formed and the matter eventually falls onto the black hole. Although this scenario can be called standard, the evidence for both accretion disks and SBHs in AGNs is only indirect (Frank, King, & Raine 1985; Blandford, Netzer, & Woltjer 1990; Falcke et al. 1993). The best evidence comes from studies of the central surface brightness of the nuclei, stellar velocity dispersion, spatial distribution of stars and X-ray emission (Young et al. 1978; Sargent et al. 1978; Binney & Tremaine 1987; Dressler & Richstone 1988, 1990; Kormendy 1988a, b; Halpern & Filippenko 1988; Dressler 1989). General relativistic effects may have important consequences for the axial symmetry and stability of accretion disks (Bardeen & Petterson 1975; Abramowicz 1987). However, the presence of black holes in AGNs is largely masked by violent plasma processes in the surrounding medium. Electromagnetic models of energy extraction assume that the SBH rotates (Blandford & Znajek 1977; Macdonald & Thorne 1982; Phinney 1983; Kaburaki & Okamoto 1991; Okamoto & Kaburaki 1991 and references cited therein). In this scenario, the energy of an AGN comes, at least partially, from the rotational energy of the SBH. Evolution of the angular momentum of the black hole under such a process was studied by Park & Vishniac (1989). It appears that the angular momentum determines the energy output of the AGN in a nontrivial manner, with the maximum at some particular value (Bičák & Janiš 1985). Unfortunately, it is unclear how the value of the angular momentum of the SBH could be determined by an independent observation. The present paper deals with this problem.

It has been proposed that a star could be captured in a bound orbit around the SBH by the tidal distortion and associated dissipation of energy (Fabian, Pringle, & Rees 1975; Frank & Rees 1976; Press & Teukolsky 1977; Lee & Ostriker 1986; Rees 1988), by tidal disruption of a binary star (Hills 1988) or a cluster (Novikov, Pethick, & Polnarev 1992), or by cumulative effects of interactions with an accretion disk (Syer, Clarke, & Rees 1991). Various aspects of star-disk collisions were studied by Ostriker (1983), Zentsova (1983), Syer et al. (1991), Zurek, Siemiginowska, & Colgate (1992), Sikora & Begelman (1992), and Vokrouhlický & Karas (1993). We assumed that the SBH forms such a binary system with a low-mass star in an orbit inclined with respect to the plane of an accretion disk. The disk is presumably thin, and its axis is aligned with the rotation axis of the black hole (Bardeen & Petterson 1975; Kumar & Pringle 1985), but the model can easily be generalized to a more complicated geometry. Radiation from the disk is periodically modulated each time the star crosses the disk. We did not attempt to specify any particular mechanism of the modulation. We also ignored secular changes of the orbital parameters of the star due to collisions with the disk and corresponding contributions of the collisions to the precession frequency. We concentrated on a gravitomagnetically induced precession of the orbit of the star. This precession is a general relativistic effect; it occurs if the central black hole rotates, and it becomes important when the star revolves close to it. In particular, we attempted to pick up relevant frequencies in the power spectrum of the simulated signal which are independent of very complex and poorly understood details of the star-disk interaction. Given the model of interaction, our approach can easily be adapted. We took into account all the relativistic effects affecting the motion and energy of photons arriving from the source to a distant observer.

We assume that the star moves along a geodesic around a Kerr black hole. The gravitomagnetic effect was originally treated by Lense & Thirring (1918) in the weak-field limit and by Wilkins (1972) in the case of a spherical orbit, r = constant, around a black hole with the extreme value of the angular momentum parameter, $a = 1$. According to our knowledge, a generalization to an eccentric and inclined orbit around a black hole with arbitrary value of the parameter $a \in (0, 1)$ has not yet been discussed in the literature. As a consequence of the gravitomagnetic effect, orbital nodes are dragged in the sense of rotation of the black hole. This dragging affects the position of the source with respect to a distant observer. We try to *extract the information which might help us to determine whether the central SBH rotates or not—provided that other details of*

[1] Astronomical Institute, Charles University, Švédská 8, 15000 Prague, Czech Republic; e-mail: jana@aci.cvut.cz; davok@aci.cvut.cz.
[2] Scuola Internazionale Superiore di Studi Avanzati, Strada Costiera 11, 34014 Trieste, Italy.

star-disk collisions are known. The weak-field limit of the angular velocity of the gravitomagnetic dragging is

$$\tilde{\Omega}_{\rm LT} \simeq 4 \times 10^5 \frac{M_\odot}{M} \frac{a}{r^3} \, {\rm s}^{-1} , \tag{1}$$

where r and a are the radius of the orbit and the angular momentum parameter of SBH measured in dimensionless geometrized units, $r = 6.7 \times 10^{-4}$ ($\tilde{r}$/1 cm). Several experiments to confirm the dragging effect in the limit of a weak gravitational field have been proposed, but they have not been carried out as yet (Everitt 1974; Braginskij, Polnarev, & Thorne 1984; Ciufolini 1986; Will 1993). The strong-field regime of the spin-orbital interaction is also intensively investigated for a relatively broad class of gravity theories within the framework of the parameterized post-Keplerian formalism. The main applications of this approach are directed at the interpretation of the binary pulsar data (e.g., Damour & Taylor 1992). Although not yet confirmed by direct observations, the gravitomagnetic effect is considered as a firm consequence of general relativity. In the strong-field region close to the black hole the gravitomagnetic precession depends on four parameters: the pericenter distance of the orbit, the eccentricity of the orbit, the inclination with respect to the equatorial plane of the black hole, and, of course, the angular momentum parameter. The above-mentioned processes of tidal interaction can set the star on an initially very eccentric trajectory, and we therefore could not restrict ourselves to circular orbits. Star-disk collisions (Syer et al. 1991; Vokrouhlický & Karas 1993), tidal effects (Press, Wiita, & Smarr 1975; Lecar, Wheeler, & McKee 1976; Boyle & Walker 1986; Zahn 1977, and 1989; Zahn & Bouchet 1989; Tassoul 1988), and gravitational radiation (Peters & Mathews 1963; Zel'dovich & Novikov 1971) tend gradually to circularize the elliptic orbit, however. Naturally, these effects modify the precession frequency, but we assumed that the star is a dwarf or a low-mass compact object and ignored the corrections. We also ignore all possible effects of the magnetic field on the spacetime geometry. For the discussion of exact solutions of Einstein-Maxwell equations describing a black hole in a magnetic field cf. Ernst (1976), Karas (1991), Manko & Sibgatullin (1992), and references cited therein.

In other words, we ignored all effects which could induce the precession of the star's orbit except the gravitomagnetic effect. We believe it is an appropriate approach in solving the problem if these effects (like star-disk interactions or gravitational radiation) are also weak. We will discuss other effects elsewhere, so that the whole subject is treated in steps.

We determined the value of the precession frequency (or, alternatively, the nodal shift per revolution, $\delta\phi$) by direct integration of the geodesic equation in terms of elliptic integrals. Gravitational radiation losses can be neglected provided that the change of the energy is small; for a circular orbit with energy $\mathscr{E}$ one obtains the dimensionless estimate (e.g., Rees, Ruffini, & Wheeler 1974)

$$|\dot{\mathscr{E}}|_{\rm grav} \approx 6.4 \left(\frac{M}{r}\right)^5 \left(\frac{M_*}{M}\right)^2 \ll 1 , \tag{2}$$

where M_* is the mass of the star. Suppose we estimate M, r, and an upper limit on the change of orbital period, $\dot{P}$, from observation. Then equation (2) provides us with the upper limit on the mass of the companion star. Analogously, if R_* is the radius of the star, one can obtain a constraint on the pericenter distance R_p which is based on the tidal limit (Carter & Luminet 1983; Luminet & Marck 1985; Rees 1988):

$$R_p \gg R_* \left(\frac{M_*}{M}\right)^{1/3} . \tag{3}$$

This paper is organized as follows. In § 2 we derive the azimuthal shift of orbital nodes. An unambiguous value can only be given in the case of spherical trajectories. The shift oscillates between the maximum and the minimum values, $\delta\phi_{\rm max}$ and $\delta\phi_{\rm min}$, if the orbit is eccentric. We define a suitable probability distribution for $\delta\phi$ and compute, numerically, a mean value $\langle\delta\phi\rangle$ which determines the gravitomagnetic precession averaged over a large number of revolutions of the star on an eccentric trajectory around the SBH. Corresponding formulae are rather complex, and, therefore, we also present a table of numerical values in the Appendix. In § 3 we present simple examples to illustrate how the gravitomagnetic frequency could be extracted from observational data. (In the present contribution we use simulated data from a simple model rather than real data.) Naturally, the frequency cannot be too small, so that the data cover at least several periods if the effect is to be detectable. The estimate of the time interval between successive collisions with the disk (see eq. [20] below) leads us to assume that the star crosses the accretion disk near the horizon (typically a few tens of the gravitational radius of the SBH) in the region where the collisions can modulate the disk radiation in the optical/X-ray bands. Possible physical mechanisms for the modulation were discussed by Mushotzky (1982); Guilbert, Fabian, & Ross (1982) and Zentsova (1985). The flux of radiation is modulated by the orbital period (short timescale) and by the perihelion shift and the Lense-Thirring period (long timescale). In order to compute observable effects, we consider both the time delay and the focusing of photons coming from the disk region to a distant observer. The focusing effect strongly enhances the influence of the Lense-Thirring precession for observers with large inclination (edge-on, with respect to the accretion disk).

A number of authors have considered periodic X-ray variability of AGNs from the thoeretical point of view (Abramowicz et al. 1989, 1992, 1993; Done et al. 1990; Honma et al. 1991; Wallinder 1991, 1992; Abramowicz 1992; Bao 1992a, b; Sikora & Begelman 1992; Rees 1993; Vio et al. 1993; King & Done 1993), and possible candidates were investigated observationally (Mittaz & Branduardi-Raymont 1989; Fiore, Massaro, & Barone 1992; Done et al. 1992). Although the periodic variability of AGNs has not yet been observationally confirmed, the whole concept is very important for theoretical models, and we believe that examples of periodically variable AGNs will be found when more data are carefully analyzed.

2. PRECESSION FREQUENCY: DETAILS OF THE CALCULATION

2.1. *Gravitomagnetic Precession*

Geodesic motion in the Kerr spacetime can be integrated in terms of elliptic integrals (Carter 1968). The appropriate form can be found in Vokrouhlický & Karas (1993). We use the standard notation for the Kerr metric (Bardeen 1973), and we refer the reader not familiar with the Kerr metric to this reference. We assume that the motion of the star is quasi-elliptic with the pericenter outside the black hole horizon, $r = R_+ \equiv 1 + (1 - a^2)^{1/2}$, and with positive energy, $0 < \mathscr{E} < 1$. The locations of the pericenter $r = R_p$ and the apocenter $r = R_a$ coin-

cide with the two upper roots of the polynomial

$$R(r) = (\mathscr{E}^2 - 1)r^4 + 2r^3 + [(\mathscr{E}^2 - 1)a^2 - \Phi^2 - \mathscr{Q}]r^2 + 2\mathscr{K}r - a^2\mathscr{Q}\,, \quad (4)$$

where $\mathscr{E} \equiv -p_t$, $\Phi \equiv p_\phi$, and $\mathscr{K}$ are the usual constants of motion, and $\mathscr{Q} \equiv \mathscr{K} + (\Phi - a\mathscr{E})^2$. In our case, all roots of $R(r)$ are real. We denote them by $R_a \geq R_p \geq R_3 \geq R_4$; $R_3 > R_+$. Other possible combinations—e.g., two complex conjugate roots—are excluded by our previous assumptions on energy and location of the pericenter above the horizon (Stewart & Walker 1973). We further assume that the star periodically crosses the equatorial plane, $\theta = \pi/2$; latitudinal motion is restricted by $|\cos\theta| \leq \mu_-$, where μ_- is the lower of the two positive roots $\mu_\pm$ of the polynomial

$$\Theta(\mu) = a^2(1 - \mathscr{E}^2)\mu^4 - [\mathscr{Q} + a^2(1 - \mathscr{E}^2) + \Phi^2]\mu^2 + \mathscr{Q}\,. \quad (5)$$

For $r \gg R_+$ one can interpret arc cos μ_- as the inclination of stellar orbit.

A nonequatorial geodesic around a rotating black hole is not planar; intersections with the $\theta = \pi/2$ plane are dragged in the sense of rotation. At first, we apply the mapping

$$[r, \phi, t, \text{sign } (\dot{r})]_n \rightarrow [r, \phi, t, \text{sign } (\dot{r})]_{n+1}\,, \quad (6)$$

which expresses coordinates of the $(n + 1)$st intersection in terms of coordinates of the previous, nth intersection with the equatorial plane. The azimuthal shift of the orbital node $\delta\phi$ per revolution is then defined by

$$\delta\phi = \phi_{n+2} - \phi_n - 2\pi \quad (7)$$

[the ϕ-coordinate is not restricted to $(0, 2\pi)$ in this convention]. One can find

$$r_{n+1} = \frac{(R_a - R_3)R_p + (R_a - R_p)R_3\sigma}{R_a - R_3 - (R_a - R_p)\sigma}\,, \quad (8)$$

$$\phi_{n+1} - \phi_n = [2(a\mathscr{E} - \Phi)A_+ + \Phi B_+]I_+ + [2(a\mathscr{E} - \Phi)A_- + \Phi B_-]I_- + \Phi J_\mu\,, \quad (9)$$

$$t_{n+1} - t_n = \mathscr{E}(J_r + 2K_r) + 2[B_+R_+\mathscr{E} + a(a\mathscr{E} - \Phi)A_+]I_+ + 2[B_-R_-\mathscr{E} + a(a\mathscr{E} - \Phi)A_-]I_- + 4\mathscr{E}I_r + a^2\mathscr{E}K_\mu\,. \quad (10)$$

We denoted

$$\sigma = \text{sn}_v^2\,(u, k_1)\,, \quad (11)$$

$$u = \tfrac{1}{2}[(R_a - R_3)(R_p - R_4)(1 - \mathscr{E}^2)]^{1/2}(I_\mu - \tilde{I}_r)\,, \quad (12)$$

$$k_1 = \frac{(R_a - R_p)(R_3 - R_4)}{(R_a - R_3)(R_p - R_4)}\,,$$

$$A_\pm = \pm\frac{R_\pm}{R_+ - R_-}\,, \quad B_\pm = \pm\frac{2R_\pm - a^2}{R_+ - R_-}\,,$$

$$R_\pm = 1 \pm (1 - a^2)^{1/2}\,,$$

$$I_\mu = \frac{2}{a\mu_+(1 - \mathscr{E}^2)^{1/2}}\,K\!\left(\frac{\mu_-}{\mu_+}\right), \quad (13)$$

$$I_\pm = \kappa_\pm[(R_p - R_3)\Pi(\varphi, n_\pm, k_1) + (R_\pm - R_p)F(\varphi, k_1)] + \tilde{I}_\pm\,, \quad (14)$$

$$n_\pm = \frac{(R_p - R_a)(R_\pm - R_3)}{(R_a - R_3)(R_\pm - R_p)}\,;$$

$F(\varphi, k)$ is the incomplete elliptic integral of the first kind, $K(k) \equiv F(\pi/2, k)$ is the corresponding complete integral and sn (u, k) is the Jacobian elliptic function (e.g., Byrd & Friedman 1971; Gradshteyn & Ryzhik 1980). Analogously, $\Pi(\varphi, n, k)$ is the elliptic integral of the third kind. In equations (8)–(10),

$$J_r + 2K_r = \kappa R_p\left[\left(\frac{R_p\alpha_1^4}{\alpha^4} + 2\frac{\alpha_1^2}{\alpha^2}\right)U + 2\frac{\alpha^2 - \alpha_1^2}{\alpha^2}\,V_1 + 2R_p\alpha_1^2\frac{\alpha^2 - \alpha_1^2}{\alpha^4}\,V_1 + R_p\frac{(\alpha^2 - \alpha_1^2)^2}{\alpha^4}\,V_2\right] + \tilde{J}_r + 2\tilde{K}_r\,, \quad (15)$$

with U, V_1, and V_2 defined by

$$U = F(\varphi, k_1)\,,$$

$$V_1 = \Pi(\varphi, -\alpha^2, k_1)\,,$$

$$V_2 = \frac{1}{2(\alpha^2 - 1)(k_1^2 - \alpha^2)}\left[\alpha^2E(\varphi, k_1) + (2\alpha^2k_1^2 + 2\alpha^2 - \alpha^4 - 3k_1^2)V_1 + (k_1^2 - \alpha^2)U - \text{sn}\,(U, k_1)\,\text{cn}\,(U, k_1)\,\text{dn}\,(U, k_1)\,\frac{\alpha^4}{1 - \alpha^2\,\text{sn}^2\,(U, k_1)}\right],$$

and

$$\alpha^2 = \frac{R_a - R_p}{R_a - R_3}\,, \quad \alpha_1^2 = \frac{R_3(R_a - R_p)}{R_p(R_a - R_3)}\,,$$

$$\sin^2\varphi = \frac{(R_a - R_3)(r_n - R_p)}{(R_a - R_p)(r_n - R_3)}\,,$$

$$\kappa = \frac{2}{[(R_1 - R_3)(R_2 - R_4)(1 - \mathscr{E}^2)]^{1/2}}\,,$$

$$\kappa_\pm = \frac{\kappa}{(R_\pm - R_3)(R_p - R_\pm)}\,.$$

$E(\varphi, k)$ denotes the incomplete elliptic integral of the second kind, cn (u, k) and dn (u, k) are the Jacobian elliptic functions,

$$J_\mu = \frac{2}{a\mu_+(1 - \mathscr{E}^2)^{1/2}}\,\Pi\!\left(-\mu_-^2, \frac{\mu_-}{\mu_+}\right), \quad (16)$$

$$K_\mu = \frac{2R_a}{a(1 - \mathscr{E}^2)^{1/2}}\left[K\!\left(\frac{\mu_-}{\mu_+}\right) - E\!\left(\frac{\mu_-}{\mu_+}\right)\right], \quad (17)$$

and $\Pi(n, k) \equiv \Pi(\pi/2, n, k)$. $\tilde{I}_r$, $\tilde{I}_\pm$, $\tilde{J}_r$, and $\tilde{K}_r$, in equations (12), (14), and (15), are the integration constants. They depend on the number of turning points in the r-coordinate between successive intersections with the equatorial plane (m) and on the sign of the radial velocity [sign $(\dot{r})$] at the intersections. For example,

$$\tilde{I}_r = \kappa[mK(k_1) - \text{sign}\,(\dot{r}_{n+1})F(\varphi, k_1)]\,. \quad (18)$$

Further details of the derivation are given in the Appendix of Vokrouhlický & Karas (1993), where the orbits under consideration are called the "Case II orbits."

The above expressions can be considerably simplified in the special case of spherical orbits with the r-coordinate constant. (It can be seen that r = constant orbits do satisfy the geodesic equation due to integrability and separability of the geodesic motion in the Kerr spacetime; Chandraskhar 1983.) The gravitomagnetic precession of the spherical orbits around an extreme ($a = 1$) Kerr black hole was studied by Wilkins (1972).

One can generalize his results to the case of spherical orbits $r \equiv R_s =$ constant with an arbitrary value of the angular momentum parameter, $|a| < 1$. Taking into account equation (9), we obtain

$$(\delta\phi)_{r=R_s} = \frac{4}{a\mu_+(1-\mathscr{E}^2)^{1/2}}\left[\Phi\Pi\left(-\mu_-^2, \frac{\mu_-}{\mu_+}\right) + a\{[\mathscr{E}(r^2+a^2) - a\Phi]\Delta^{-1} - \mathscr{E}\}K\left(\frac{\mu_-}{\mu_+}\right)\right] - 2\pi , \tag{19}$$

where $\Delta = r^2 - 2r + a^2$. The corresponding orbital period is

$$P_{r=R_s} = 2\left[\frac{r^2(r^2+a^2)\mathscr{E} + 2ar(a\mathscr{E} - \Phi)}{\Delta} I_\mu + a^2\mathscr{E}K_\mu\right], \tag{20}$$

and the percession frequency is

$$(\Omega_{\rm LT})_{r=R_s} = \left(\frac{\delta\phi}{P}\right)_{r=R_s} . \tag{21}$$

Setting $a = 0$ in equations (19) and (20), one arrives at $\delta\phi = 0$ and $P = 2\pi R_s^{3/2}$, which corresponds to Keplerian motion with vanishing nodal shift in the Schwarzschild metric, as expected. On the other hand, if $a \neq 0$, the dominant term in the asymptotic expansion of equation (19) for $r \to \infty$ coincides with the well-known result of Lense & Thirring (1918): $\delta\phi = 2\pi a R_s^{-3/2}$. The dependence of period P on the inclination μ is only weak, and equation (20) can be approximated by its value for equatorial orbits:

$$P \approx 2\pi(r^{3/2} \pm a) , \tag{22}$$

where the plus and minus signs correspond to direct and retrograde orbits with respect to the rotating SBH. Analogously, the nodal shift of spherical polar orbits ($\Phi = 0$) can be obtained from equation (19) with $\mu_- = 1$. Polar orbits were studied by Stoghianidis & Tsoubelis (1987).

2.2. *Motion of the Pericenter*

In the present paper we are mainly interested in the frequency of the gravitomagnetic precession. In the data, however, there will also be present a periodicity associated with another relativistic effect—the pericenter shift. We thus need to estimate the corresponding precession frequency Ω_P. In the Schwarzschild case

$$\Omega_P = \delta\phi/P , \tag{23}$$

where

$$\delta\phi = \frac{4}{\omega}K(k) - 2\pi , \tag{24}$$

$$P = \left[\frac{u_2+u_1}{u_3-u_1}(1-2u_1)(1-2u_2)\right]^{1/2}\left\{\frac{4}{u_1}\Pi(\alpha^2, k') + \frac{8}{1-2u_1}\Pi\left(2\frac{u_2-u_1}{1-2u_1}, k'\right) + \frac{1}{u_1^2\alpha^2(k'^2-\alpha^2)}[\alpha^2E(k') + (k'^2-\alpha^2)K(k') + (2\alpha^2k'^2 + 2\alpha^2 - \alpha^4 - 3k'^2)\Pi(\alpha^2, k')]\right\} . \tag{25}$$

Here

$$\omega = (1 - 2u_2 - 4u_1)^{1/2} , \quad k^2 = 2(u_2 - u_1)\omega^{-2} ,$$

$$\alpha^2 = 1 - \frac{u_2}{u_1} , \quad k'^2 = \frac{u_2 - u_1}{u_3 - u_1} ,$$

where $u_1 \equiv 1 - R_a$, $u_2 \equiv 1/R_p$ and $u_3 = \frac{1}{2} - u_1 - u_2$ are roots of the polynomial in $u = 1/r$:

$$U(u) = 2u^3 - u^2 + 2\mathscr{L}^{-2}u - (1 - \mathscr{E}^2)\mathscr{L}^{-2}$$

(cf. "Case I orbits" in Appendix of Vokrouhlický & Karas 1993). The angular momentum $\mathscr{L}$ is defined with respect to the axis perpendicular to the orbital plane of the star, not with respect to the axis of the disk like Φ in the Kerr case. This definition is naturally more advantageous in the Schwarzschild case because the orbit is planar.

An analogous effect of the pericenter shift can be expected in the Kerr case, too. Now, however, there is no unambiguous value of Ω_P because the orbit does not remain planar and the pericenter shift is mixed up with gravitomagnetic precession. We calculate Ω_P numerically by applying the mapping algorithm (6) for the r-coordinate over a large number of revolutions of the star around the SBH.

2.3. *The Mean Value of the Precession Frequencies*

A specific value of the nodal shift $\delta\phi$ and the corresponding precession frequency can only be associated with spherical orbits. In this case $\delta\phi$ is specified by equation (19) with three parameters—a, μ_-, and R_s. The case of a quasi-elliptic orbit with nonzero eccentricity requires knowledge of four parameters. The appropriate parameters are a, μ_-, pericenter distance R_p, and eccentricity $e \equiv (R_a - R_p)/(R_a + R_p)$. The nodal shift oscillates between the maximum and the minimum values, $\delta\phi_{\rm max}$ and $\delta\phi_{\rm min}$. Figures 1 and 2 show the graphs of $\delta\phi(r)$ for some typical values of the parameters (here r denotes the radius of the intersection with the equatorial plane). For practical purposes one needs the mean value of the shift which characterizes an average taken over a large number of revo-

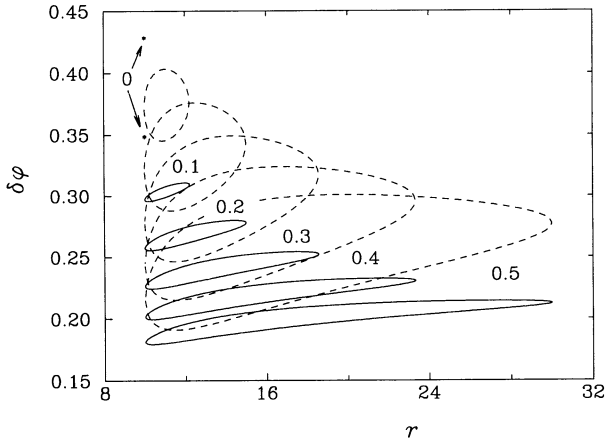

FIG. 1.—Nodal shift $\delta\phi(r)$ (in radians) per revolution for different eccentricities of the orbit as a function of the radial distance of the intersection with the equatorial plane. Solid lines correspond to direct orbits; dashed lines correspond to retorgrade orbits. Numbers given with each curve indicate the eccentricity. The inclination parameter is arc cos $\mu_- = 45°$, $a = 0.9981$. Two values of $\delta\phi$ for given r correspond to $\dot{r} > 0$ and $\dot{r} < 0$, respectively. The case of spherical orbits is denoted by an asterisk.

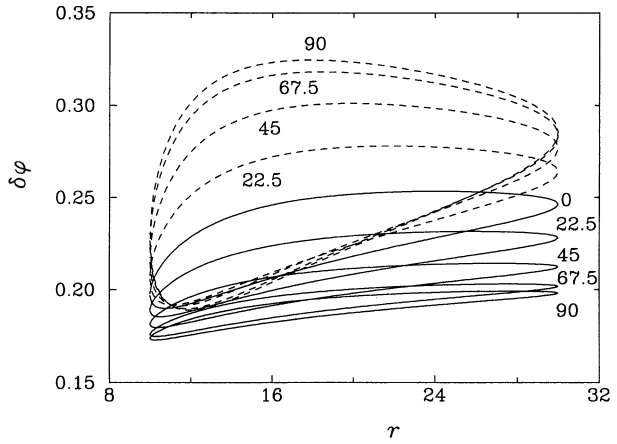

FIG. 2.—As in Fig. 1, but for different inclinations and constant eccentricity. Now $e = 0.5$, and the numbers indicate the value of arc cos μ_- in degrees. In particular, arc cos $\mu_- = 90°$ corresponds to equatorial orbits. Naturally, the curves of direct and retorgrade polar orbits (arc cos $\mu_- = 0$) coincide.

lutions. We define

$$\langle \delta\phi \rangle = \int_{R_p}^{R_a} \delta\phi(x)\mathscr{P}(x)|_{\mathscr{E},\Phi,\mathscr{Q},a}\, dx\,, \tag{26}$$

where $\mathscr{P}(r)$ is the probability distribution for the radial coordinate of the intersections of the specified trajectory with the disk. $\mathscr{P}$ is normalized to unity, $\int P(x)\, dx = 1$. We applied the following numerical procedure for evaluating equation (26): (1) at first, for a given set of orbital parameters ($\mathscr{E}$, Φ, $\mathscr{Q}$), we constructed the probability distribution by following the course of an ensemble of orbits with identical orbital parameters and randomly chosen initial conditions; (2) we then applied equation (7) and performed the integration in equation (26). The resulting values of the mean nodal shift are tabulated in the Appendix. One can see that the dispersion is often quite small, and the mean value is a satisfactory approximation to the current value of $\delta\phi$, except for very close orbits.

Analogously to $\langle \delta\phi \rangle$, we introduce the mean orbital period $\langle P \rangle$ of an eccentric orbit, and we calculate $\langle \Omega_P \rangle$ by applying the mapping algorithm in equation (6) for the r-coordinate over a large number of revolutions of the star around the SBH.

3. NUMERICAL MODELS

In this section we will show how the relativistic precession becomes evident in a simulated signal from the source. We take into account general relativistic effects on photons coming from the source to the observer with no approximation. The method for integrating light trajectories in the Kerr metric has been discussed by many authors (Cunningham & Bardeen 1973; de Felice, Nobili, & Calvani 1974; Cunningham 1975, 1976; Asaoka 1989). We employ an efficient approach described by Karas, Vokrouhlický, & Polnarev (1992). We do not include the noise component which is of course present in a real signal. The reason is that the form of the noise depends on its particular model, and it does not affect the periodicities we are interested in. The way to account for the noise in the synthetic light curve is straightforward, in principle, if one adopts a specific model of its origin. Such a model can be based on mechanisms proposed by Moskalik & Sikora 1986; Chagelishvili, Lominadze, & Rogava 1989, Abramowicz et al. 1991, or Baring 1992.

The position of a distant observer is characterized by his inclination, θ_o, with respect to the symmetry axis. We assume that the star-disk collisions modulate the disk radiation at the moment when the star crashes through the disk from the far side to the near side with respect to the observer, i.e., once per revolution. The light travel time to the observer depends on the location of the intersection, and it is thus periodically affected by the precession. Frequencies corresponding to the periodic modulation of the signal are evident in the Fourier transform of arrival times.

The lensing effect enhances the radiation when the source is behind the black hole and thus contributes to the periodic modulation of the signal. As an alternative to the previously described Fourier transform of arrival times, one can detect frequencies in the power spectrum of the photometric radiative flux. However, in this alternative approach the input signal for the Fourier transform depends on the model of the star-disk interaction (see below). We assume, for simplicity, that the shape of the observed signal from successive collisions has always an identical profile: a sharp onset and then an exponential decrease of the local luminosity in the static frame or, alternatively, in the disk co-rotating frame. In the latter case both the lensing and the Doppler effect contribute to the signal strength. Figure 3 is an example of typical light curves. We assumed a spherical orbit, $r = 6$, around a nearly extreme Kerr black hole. It is not clear whether such a close orbit is astrophysically realistic because the process of capture is not well understood (Rees 1993). A more plausible configuration is demonstrated in Figure 7.

The basic frequency in the power spectrum of the observed signal corresponds to the orbital motion. One can detect two fundamental lines in the power spectrum. The first line, at higher frequency ($\Omega_o = 2\pi/P$; see eq. [20]), corresponds to the orbital motion, and the second one, at lower frequency (Ω_{LT}; see eq. [21]), corresponds to the gravitomagnetic precession. Figure 4 shows the normalized power spectrum of the light curve from the previous figure, strictly speaking the coefficient of spectral correlation as defined by Ferraz-Mello (1981). The power spectrum also contains linear combinations of fundamental frequencies.

The shape of the light curve naturally depends on the particular model and position of the observer; however, we expect that identical periodicities caused by the precession of the orbit will be present in the signal independently of the details. The power spectrum constructed from arrival times has simple form. In Figure 5 we applied the Fourier transform on time intervals elapsed between successive flares in the light curve. Now the shape of the spectrum is determined by orbital parameters of the star and angular momentum of the SBH, but it depends only very weakly on other details of the model—decay time of the flare, viewing angle of the observer, etc. This advantageous property is easy to understand because the arrival times of succesive flares are directly related to the precession of the orbit, and we thus avoid the model-dependent features in the light curve.

As mentioned above, several effects tend to circulate the orbit of the star, and for this reason spherical orbits are of special interest. However, the star can initially be captured in an eccentric orbit. Therefore, we also considered the case of quasi-elliptic orbits ($e \neq 0$). The pericenter shift reveals itself as another line in the power spectrum. In Figure 6 one can detect lines corresponding to the orbital motion (Ω_o), the gravitomagnetic precession (Ω_{LT}), and the pericenter shift (Ω_P). The gravitomagnetic precession disappears in the Schwarzschild

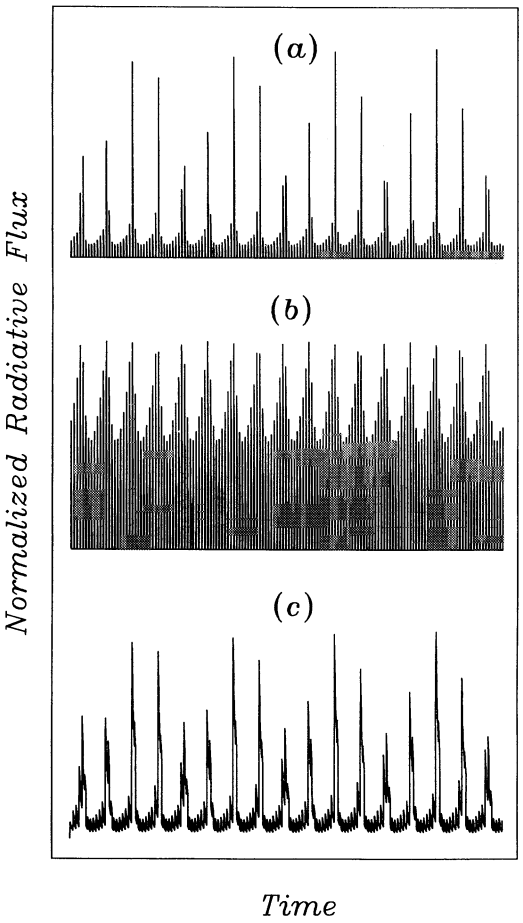

FIG. 3.—Numerical simulation of the observed light curve. Radiative flux is given in arbitrary units on the ordinate. The flux is periodically affected by the lensing effect (main peaks) when the source of radiation is behind the black hole. In this example we consider a source of radiation which is located in the equatorial plane in the place where the star intersected the disk. The position of the intersection is affected by the gravitomagnetic precession, provided that the central supermassive black hole rotates. As a consequence, the places of intersection are dragged in the azimuthal direction; the figure covers 17 periods. The luminosity of the source is isotropic in the locally static frame and decreases exponentially with e-folding time τ. The position of the observer at infinity is characterized by the viewing angle θ_o; $\theta_o = 0$ is the rotation axis of the black hole. The angular momentum parameter is chosen to be $a = 0.9981$. The star moves in an inclined spherical orbit: $r = 6$, $\mu_- = 0.5$. The three cases correspond to (*a*) $\theta = 80°$, $\tau = 0.2P$, (*b*) $\theta = 40°$, $\tau = 0.2P$, (*c*) $\theta = 80°$, $\tau = 1.5P$, where $P|_{r=6}$ is the orbital period given by eq. (22). Further details of the model are described in the text.

case, and the power spectrum of an eccentric orbit is then rather similar to the case of a spherical orbit near a Kerr black hole. To distinguish between the two extreme cases, one needs an independent estimate of the radius and eccentricity of the orbit (Fig. 7).

4. CONCLUSIONS

We considered the general relativistic precession of a star orbiting a supermassive black hole and colliding with an accretion disk in the nucleus of an AGN. We derived formulae for the azimuthal shift due to the gravitomagnetic precession and perihelion shift during the free (geodesic) part of the motion between subsequent interactions with the accretion disk. No restrictions on the orbital parameters and the black hole angular momentum were imposed, except that they describe a stable bound trajectory around the Kerr black hole. Within the framework of this model our results restrict possible values of the angular momentum of the central black hole. To illustrate the precession effect, we adopted a simplified model of the star-disk interaction, and we determined relevant frequencies in the power spectrum of the observed signal. Both types of the relativistic precession which are relevant for our problem—the precession related to the pericenter shift and the gravitomagnetic (Lense-Thirring) precession—expose themselves clearly in the power spectrum. We found the analysis of arrival times conceptually more trivial and at the same time more advantageous than the analysis of the complete photometric curve.

Our conjecture is that the typical character of the power spectrum will remain conserved at some level in astrophysically more realistic models of the interaction. Such an assumption is well founded provided that the orbital parameters of the star are not changed significantly during several periods associated with the precession motion ($\Omega_o \gg \Omega_{LT}, \Omega_P$). More realistic models must include the effects of tidal interactions, gravitational radiation, and star-disk collisions on the orbital parameters (work in preparation).

We thank M. Abramowicz, C. Done, and A. Lanza for very useful discussions concerning the problem of AGN variability, and P. Haines for a careful reading of the manuscript. We also thank the unknown referee and participants in the Relativity Seminar in Prague for comments and suggestions that helped us to improve our work.

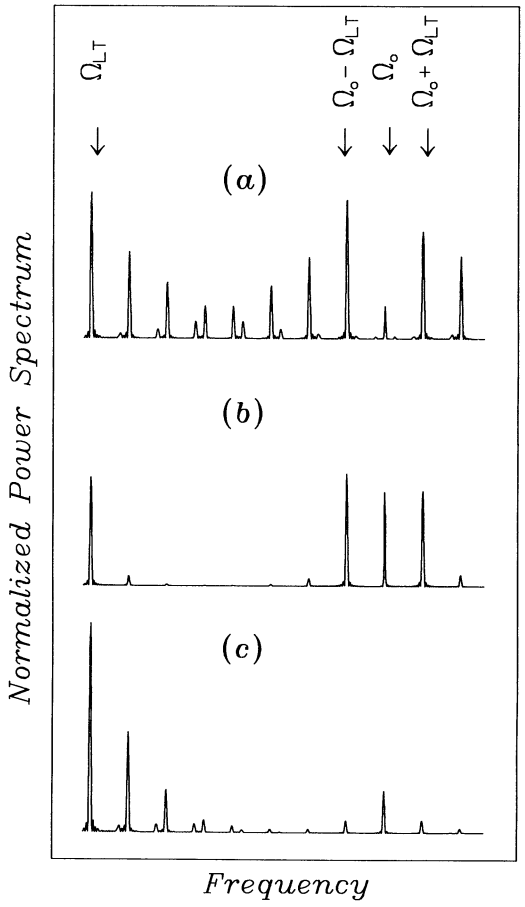

FIG. 4.—Normalized power spectrum of the light curve from Fig. 3. The coefficient of spectral correlation is the ordinate, and the spectral wind is the abscissa.

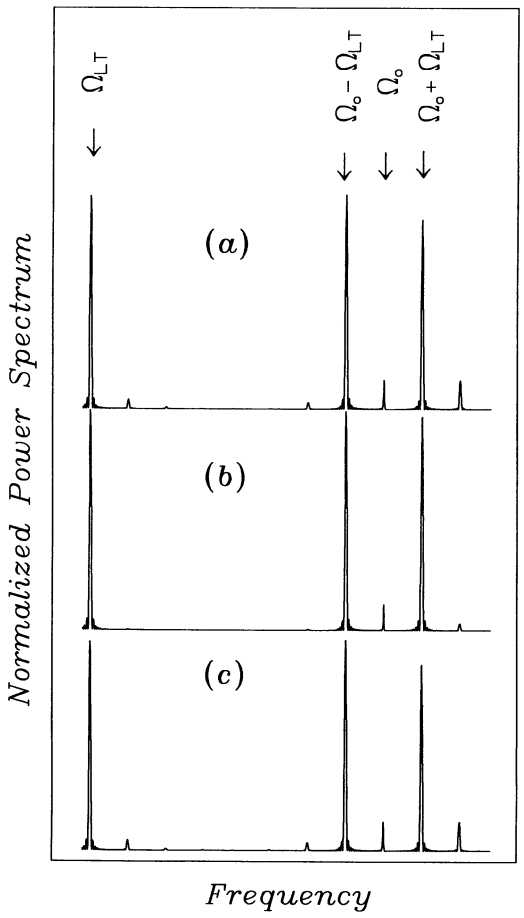

FIG. 5.—Normalized power spectrum of the arrival times for the signal from Fig. 3. The axes are as in Fig. 4. One can verify that the typical shape of the spectrum is quite insensitive to the details of configuration in a broad range of parameters.

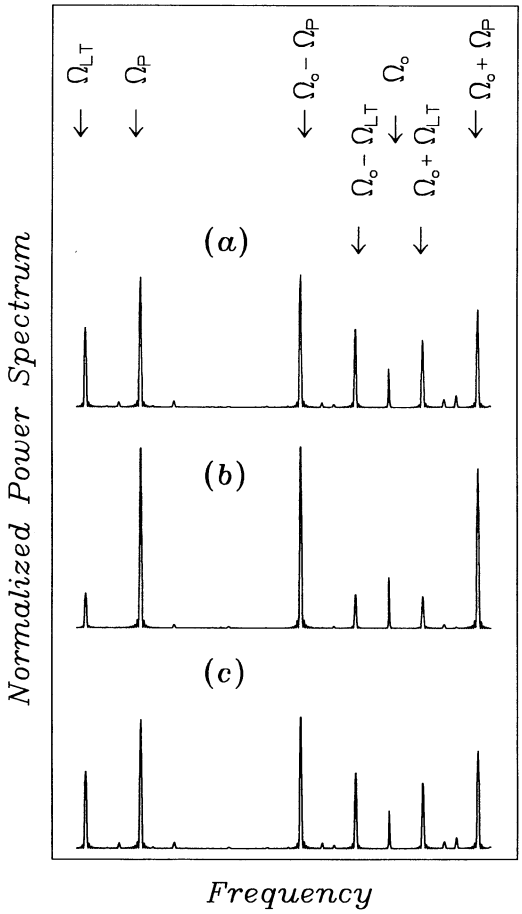

FIG. 6.—As in Fig. 5. The orbit of the star is now eccentric: $e = 0.1$, $R_p = 6$, $\mu_- = 0.5$. Parameters of the three cases (*a*)–(*c*) as before.

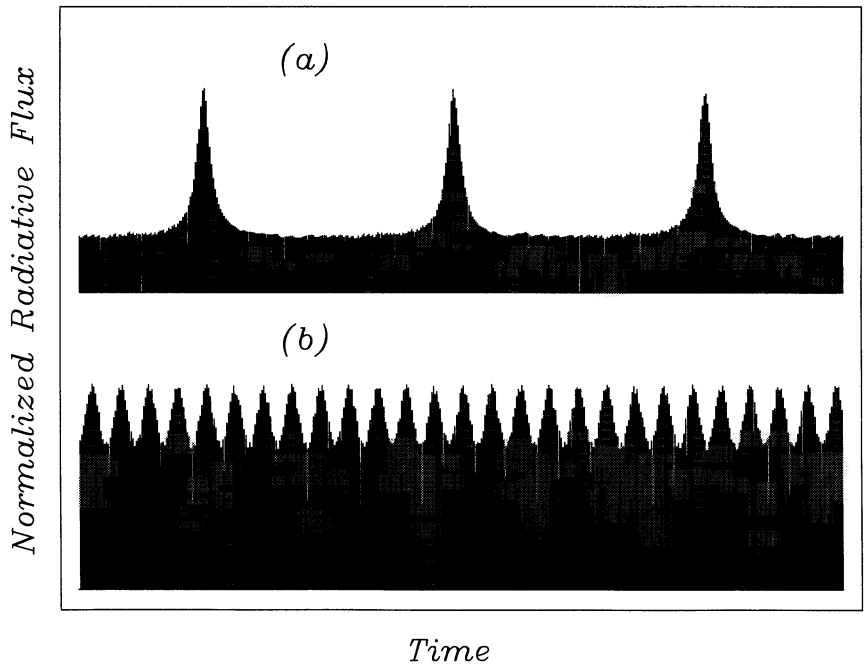

FIG. 7.—Calculated light curves for the simple model described in § 3. Case *a* is for the Kerr black hole with $a = 0.9981$ and a circular trajectory of the star at $R_s = 40$. The long-term modulation of the light curve (three main peaks) is due to the gravitomagnetic precession (angular frequency Ω_{LT}). Case *b* is for a nonrotating black hole and an eccentric trajectory ($e = 0.25$, $R_p = 40$). Now the modulation is due to the pericenter shift, and it has a different period which is given by $\langle \Omega_P \rangle$.

APPENDIX

We tabulate the azimuthal shift of orbital nodes due to the gravitomagnetic precession. The three tables correspond to $a = 0.33$ (Table 1), $a = 0.67$ (Table 2), and $a = 1$ (Table 3). In the tables, R_p denotes the pericenter distance in units of the gravitational radius R_+, e is the eccentricity of the orbit, and μ_- is the parameter characterizing inclination in the asymptotic region, $r \gg R_+$ (see eq. [5]). The columns headed " + " and " − " correspond to direct ($\Phi > 0$) and retrograde ($\Phi < 0$) orbits, respectively. (The difference

TABLE 1

NODAL SHIFT DUE TO GRAVITOMAGNETIC PRECESSION: $a = 0.33$

R_p	$e \rightarrow$	0.		.2		.4		.6		.8	
↓	$\mu_- \downarrow$	+	−	+	−	+	−	+	−	+	−
	0.	1311 ± 0	1441 ± 0	1005 ± 69	1110 ± 126	810 ± 89	900 ± 156	677 ± 92	754^{+155}_{-159}	580 ± 89	648^{+145}_{-151}
	.25	1313 ± 0	1439 ± 0	1006 ± 70	1109 ± 125	812 ± 90	898^{+154}_{-156}	678 ± 93	753^{+154}_{-157}	581 ± 90	647^{+144}_{-150}
5	.5	1321 ± 0	1434 ± 0	1012 ± 72	1104 ± 121	816 ± 92	894^{+150}_{-152}	682^{+95}_{-97}	749^{+150}_{-153}	585^{+92}_{-94}	643^{+140}_{-146}
	.75	1336 ± 0	1422 ± 0	1024 ± 77	1093 ± 114	826 ± 98	885^{+142}_{-144}	690 ± 101	741^{+142}_{-146}	592^{+97}_{-99}	636^{+134}_{-139}
	1.	1381 ± 0		1059 ± 94		856^{+118}_{-120}		715^{+120}_{-123}		614^{+114}_{-118}	
	0.	466 ± 0	510 ± 0	356 ± 10	389 ± 15	285 ± 13	310 ± 20	236 ± 14	256 ± 20	200 ± 14	217 ± 20
	.25	467 ± 0	509 ± 0	357 ± 10	388 ± 15	286 ± 14	310 ± 20	236 ± 14	256 ± 20	201 ± 14	217 ± 19
10	.5	469 ± 0	507 ± 0	359 ± 10	387 ± 15	287 ± 14	309 ± 19	238 ± 15	255 ± 20	201 ± 14	216 ± 19
	.75	474 ± 0	503 ± 0	362 ± 11	383 ± 14	290 ± 14	306 ± 19	240 ± 15	253 ± 19	203 ± 15	214 ± 18
	1.	488 ± 0		373 ± 13		298 ± 16		246 ± 17		209 ± 17	
	0.	255 ± 0	276 ± 0	195 ± 3	210 ± 5	156 ± 5	167 ± 6	129 ± 5	138 ± 7	109 ± 6	116 ± 6
	.25	256 ± 0	276 ± 0	195 ± 4	210 ± 5	156 ± 5	167 ± 6	129 ± 5	137 ± 7	109 ± 5	116 ± 6
15	.5	257 ± 0	275 ± 0	196 ± 4	209 ± 5	157 ± 5	167 ± 6	129 ± 5	137 ± 7	109 ± 5	116 ± 6
	.75	259 ± 0	273 ± 0	198 ± 4	208 ± 5	158 ± 5	165 ± 6	130 ± 5	136 ± 6	110 ± 5	115 ± 6
	1.	266 ± 0		203 ± 4		162 ± 6		133 ± 6		112 ± 6	
	0.	166 ± 0	179 ± 0	127 ± 2	136 ± 2	101 ± 2	108 ± 3	84 ± 2	89 ± 3	70 ± 2	75 ± 3
	.25	167 ± 0	179 ± 0	127 ± 2	136 ± 2	102 ± 2	108 ± 3	84 ± 2	89 ± 3	71 ± 2	75 ± 3
20	.5	167 ± 0	178 ± 0	128 ± 2	135 ± 2	102 ± 2	108 ± 3	84 ± 2	88 ± 3	71 ± 2	74 ± 3
	.75	169 ± 0	177 ± 0	129 ± 2	135 ± 2	103 ± 2	107 ± 3	84 ± 3	88 ± 3	71 ± 2	74 ± 3
	1.	173 ± 0		132 ± 2		105 ± 3		86 ± 3		73 ± 3	
	0.	120 ± 0	128 ± 0	91 ± 1	97 ± 1	73 ± 1	77 ± 2	60 ± 1	63 ± 2	50 ± 1	53 ± 2
	.25	120 ± 0	128 ± 0	91 ± 1	97 ± 1	73 ± 1	77 ± 2	60 ± 1	63 ± 2	50 ± 1	53 ± 2
25	.5	120 ± 0	127 ± 0	92 ± 1	97 ± 1	73 ± 1	77 ± 2	60 ± 1	63 ± 2	51 ± 1	53 ± 2
	.75	121 ± 0	126 ± 0	92 ± 1	96 ± 1	73 ± 1	76 ± 2	60 ± 1	63 ± 2	51 ± 1	53 ± 2
	1.	124 ± 0		94 ± 1		75 ± 1		62 ± 2		52 ± 1	
	0.	91 ± 0	97 ± 0	70 ± 1	74 ± 1	55 ± 1	58 ± 1	46 ± 1	48 ± 1	38 ± 1	40 ± 1
	.25	91 ± 0	97 ± 0	70 ± 1	74 ± 1	55 ± 1	58 ± 1	46 ± 1	48 ± 1	38 ± 1	40 ± 1
30	.5	92 ± 0	96 ± 0	70 ± 1	73 ± 1	56 ± 1	58 ± 1	46 ± 1	48 ± 1	38 ± 1	40 ± 1
	.75	92 ± 0	96 ± 0	70 ± 1	73 ± 1	56 ± 1	58 ± 1	46 ± 1	48 ± 1	39 ± 1	40 ± 1
	1.	94 ± 0		72 ± 1		57 ± 1		47 ± 1		39 ± 1	
	0.	72 ± 0	77 ± 0	55 ± 0	58 ± 1	44 ± 1	46 ± 1	36 ± 1	38 ± 1	30 ± 1	32 ± 1
	.25	73 ± 0	77 ± 0	55 ± 0	58 ± 1	44 ± 1	46 ± 1	36 ± 1	38 ± 1	30 ± 1	32 ± 1
35	.5	73 ± 0	76 ± 0	56 ± 0	58 ± 0	44 ± 1	46 ± 1	36 ± 1	38 ± 1	31 ± 1	32 ± 1
	.75	73 ± 0	76 ± 0	56 ± 0	58 ± 0	44 ± 1	46 ± 1	36 ± 1	38 ± 1	31 ± 1	32 ± 1
	1.	75 ± 0		57 ± 0		45 ± 1		37 ± 1		31 ± 1	
	0.	59 ± 0	63 ± 0	45 ± 0	48 ± 0	36 ± 0	38 ± 0	30 ± 0	31 ± 0	25 ± 0	26 ± 0
	.25	59 ± 0	63 ± 0	45 ± 0	48 ± 0	36 ± 0	38 ± 0	30 ± 0	31 ± 0	25 ± 0	26 ± 0
40	.5	60 ± 0	62 ± 0	45 ± 0	47 ± 0	36 ± 0	38 ± 0	30 ± 0	31 ± 0	25 ± 0	26 ± 0
	.75	60 ± 0	62 ± 0	46 ± 0	47 ± 0	36 ± 0	38 ± 0	30 ± 0	31 ± 0	25 ± 0	26 ± 0
	1.	61 ± 0		46 ± 0		37 ± 0		30 ± 0		25 ± 0	
	0.	50 ± 0	52 ± 0	38 ± 0	40 ± 0	30 ± 0	32 ± 0	25 ± 0	26 ± 0	21 ± 0	22 ± 0
	.25	50 ± 0	52 ± 0	38 ± 0	40 ± 0	30 ± 0	32 ± 0	25 ± 0	26 ± 0	21 ± 0	22 ± 0
45	.5	50 ± 0	52 ± 0	38 ± 0	40 ± 0	30 ± 0	32 ± 0	25 ± 0	26 ± 0	21 ± 0	22 ± 0
	.75	50 ± 0	52 ± 0	38 ± 0	40 ± 0	31 ± 0	31 ± 0	25 ± 0	26 ± 0	21 ± 0	22 ± 0
	1.	51 ± 0		39 ± 0		31 ± 0		25 ± 0		21 ± 0	
	0.	43 ± 0	45 ± 0	33 ± 0	34 ± 0	26 ± 0	27 ± 0	21 ± 0	22 ± 0	18 ± 0	19 ± 0
	.25	43 ± 0	45 ± 0	33 ± 0	34 ± 0	26 ± 0	27 ± 0	21 ± 0	22 ± 0	18 ± 0	19 ± 0
50	.5	43 ± 0	45 ± 0	33 ± 0	34 ± 0	26 ± 0	27 ± 0	21 ± 0	22 ± 0	18 ± 0	18 ± 0
	.75	43 ± 0	44 ± 0	33 ± 0	34 ± 0	26 ± 0	27 ± 0	21 ± 0	22 ± 0	18 ± 0	18 ± 0
	1.	44 ± 0		33 ± 0		26 ± 0		22 ± 0		18 ± 0	

naturally disappears for polar orbits which are characterized by $\mu_- = 1$ and $\Phi = 0$.) The nodal shift is given in the form

$$\langle \delta\phi \rangle^{+(\delta\phi_{\max} - \langle \delta\phi \rangle)}_{-(\langle \delta\phi \rangle - \delta\phi_{\min})} \; [10^{-4} \text{ rad}] ,$$

where $\langle \delta\phi \rangle$ is the mean value of the shift and $\delta\phi_{\max}$, $\delta\phi_{\min}$ are the maximum and the minimum values of the shift (for details see the text). In particular, for spherical orbits (r = constant, $e = 0$) we obtain $\delta\phi_{\max} = \langle \delta\phi \rangle = \delta\phi_{\min}$; in this case, $\langle \delta\phi \rangle$ is given by equation (19). An ellipsis in Table 3 excludes those combinations of parameters which do not correspond to a timelike geodesic.

TABLE 2

NODAL SHIFT DUE TO GRAVITOMAGNETIC PRECESSION: $a = 0.67$

R_p	$e \rightarrow$	0.		.2		.4		.6		.8	
$\downarrow$	$\mu_- \downarrow$	+	−	+	−	+	−	+	−	+	−
5	0.	2883 ± 0	3480 ± 0	2212 ± 128	2721 ± 462	1787 ± 171	2229^{+565}_{-563}	1496 ± 181	1883^{+555}_{-558}	1285^{+179}_{-176}	1629^{+510}_{-524}
	.25	2895 ± 0	3474 ± 0	2221 ± 131	2713 ± 454	1794 ± 174	2221^{+556}_{-553}	1502 ± 185	1876^{+546}_{-550}	1291^{+182}_{-180}	1623^{+502}_{-516}
	.5	2935 ± 0	3453 ± 0	2251 ± 141	2689 ± 428	1818 ± 186	2199 ± 525	1522 ± 196	1855^{+517}_{-522}	1308^{+193}_{-191}	1604^{+476}_{-490}
	.75	3013 ± 0	3407 ± 0	2310 ± 163	2642 ± 381	1865 ± 212	2154 ± 468	1561 ± 222	1814^{+464}_{-470}	1341^{+215}_{-217}	1566^{+430}_{-444}
	1.	3232 ± 0		2485^{+261}_{-254}		2012^{+319}_{-322}		1687^{+323}_{-329}		1452^{+306}_{-316}	
10	0.	1035 ± 0	1246 ± 0	794 ± 21	950 ± 51	638 ± 29	760 ± 65	529 ± 31	628^{+65}_{-68}	450 ± 31	532 ± 66
	.25	1039 ± 0	1243 ± 0	797 ± 21	948 ± 51	640 ± 29	758^{+64}_{-66}	531 ± 31	626^{+65}_{-67}	452 ± 31	531^{+61}_{-65}
	.5	1050 ± 0	1233 ± 0	806 ± 22	941 ± 49	647 ± 30	752 ± 62	536 ± 33	621^{+62}_{-65}	456 ± 32	527^{+59}_{-62}
	.75	1074 ± 0	1213 ± 0	822 ± 25	925 ± 45	659 ± 33	740 ± 57	546 ± 35	612^{+58}_{-60}	464 ± 35	519^{+55}_{-58}
	1.	1146 ± 0		875 ± 34		700 ± 44		579 ± 46		491 ± 44	
15	0.	571 ± 0	674 ± 0	438 ± 8	512 ± 16	351 ± 10	408 ± 20	290 ± 11	335 ± 21	246 ± 11	283 ± 20
	.25	573 ± 0	673 ± 0	439 ± 8	511 ± 15	352 ± 10	407 ± 20	291 ± 11	334 ± 20	246 ± 11	282 ± 19
	.5	578 ± 0	668 ± 0	443 ± 8	508 ± 15	355 ± 11	404 ± 19	293 ± 12	332 ± 20	248 ± 12	280 ± 19
	.75	589 ± 0	658 ± 0	451 ± 9	500 ± 14	361 ± 12	398 ± 18	298 ± 12	328 ± 19	252 ± 12	276 ± 18
	1.	624 ± 0		476 ± 11		380 ± 15		313 ± 15		264 ± 15	
20	0.	375 ± 0	435 ± 0	287 ± 4	330 ± 7	230 ± 5	262 ± 9	190 ± 6	215 ± 9	160 ± 6	181 ± 9
	.25	376 ± 0	434 ± 0	288 ± 4	330 ± 7	230 ± 5	262 ± 9	190 ± 6	215 ± 9	161 ± 6	181 ± 9
	.5	379 ± 0	431 ± 0	290 ± 4	328 ± 7	232 ± 5	260 ± 9	191 ± 6	214 ± 9	162 ± 6	180 ± 9
	.75	385 ± 0	425 ± 0	295 ± 4	323 ± 6	235 ± 6	257 ± 8	194 ± 6	211 ± 9	164 ± 6	178 ± 8
	1.	405 ± 0		309 ± 5		246 ± 7		202 ± 7		171 ± 7	
25	0.	270 ± 0	310 ± 0	207 ± 2	235 ± 4	165 ± 3	186 ± 5	136 ± 3	153 ± 5	115 ± 3	128 ± 5
	.25	271 ± 0	309 ± 0	207 ± 2	235 ± 4	166 ± 3	186 ± 5	137 ± 3	153 ± 5	115 ± 3	128 ± 5
	.5	273 ± 0	307 ± 0	209 ± 2	233 ± 4	167 ± 3	185 ± 5	137 ± 3	152 ± 5	116 ± 3	127 ± 5
	.75	277 ± 0	303 ± 0	212 ± 2	230 ± 3	169 ± 3	183 ± 4	139 ± 3	150 ± 5	117 ± 3	126 ± 5
	1.	290 ± 0		221 ± 3		176 ± 4		145 ± 4		122 ± 4	
30	0.	207 ± 0	235 ± 0	158 ± 1	178 ± 2	126 ± 2	141 ± 3	104 ± 2	116 ± 3	88 ± 2	97 ± 3
	.25	207 ± 0	234 ± 0	158 ± 1	178 ± 2	127 ± 2	141 ± 3	104 ± 2	115 ± 3	88 ± 2	97 ± 3
	.5	208 ± 0	233 ± 0	159 ± 1	177 ± 2	127 ± 2	140 ± 3	105 ± 2	115 ± 3	88 ± 2	96 ± 3
	.75	211 ± 0	230 ± 0	162 ± 1	175 ± 2	129 ± 2	139 ± 3	106 ± 2	114 ± 3	89 ± 2	95 ± 3
	1.	221 ± 0		168 ± 2		134 ± 3		110 ± 3		92 ± 2	
35	0.	165 ± 0	186 ± 0	126 ± 1	141 ± 1	101 ± 1	112 ± 2	83 ± 1	91 ± 2	70 ± 1	77 ± 2
	.25	165 ± 0	185 ± 0	126 ± 1	140 ± 1	101 ± 1	111 ± 2	83 ± 1	91 ± 2	70 ± 1	77 ± 2
	.5	166 ± 0	184 ± 0	127 ± 1	140 ± 1	101 ± 1	111 ± 2	83 ± 1	91 ± 2	70 ± 1	76 ± 2
	.75	168 ± 0	182 ± 0	128 ± 1	138 ± 1	102 ± 1	110 ± 2	84 ± 1	90 ± 2	71 ± 1	75 ± 2
	1.	175 ± 0		133 ± 1		106 ± 2		87 ± 2		73 ± 2	
40	0.	135 ± 0	151 ± 0	103 ± 1	115 ± 1	83 ± 1	91 ± 1	68 ± 1	74 ± 1	57 ± 1	62 ± 1
	.25	136 ± 0	151 ± 0	104 ± 1	115 ± 1	83 ± 1	91 ± 1	68 ± 1	74 ± 1	57 ± 1	62 ± 1
	.5	136 ± 0	150 ± 0	104 ± 1	114 ± 1	83 ± 1	90 ± 1	68 ± 1	74 ± 1	58 ± 1	62 ± 1
	.75	138 ± 0	149 ± 0	105 ± 1	113 ± 1	84 ± 1	90 ± 1	69 ± 1	73 ± 1	58 ± 1	62 ± 1
	1.	143 ± 0		109 ± 1		87 ± 1		71 ± 1		60 ± 1	
45	0.	114 ± 0	127 ± 0	87 ± 1	96 ± 1	69 ± 1	76 ± 1	57 ± 1	62 ± 1	48 ± 1	52 ± 1
	.25	114 ± 0	126 ± 0	87 ± 1	96 ± 1	69 ± 1	76 ± 1	57 ± 1	62 ± 1	48 ± 1	52 ± 1
	.5	115 ± 0	126 ± 0	88 ± 1	95 ± 1	70 ± 1	76 ± 1	57 ± 1	62 ± 1	48 ± 1	52 ± 1
	.75	116 ± 0	124 ± 0	88 ± 1	94 ± 1	70 ± 1	75 ± 1	58 ± 1	61 ± 1	49 ± 1	51 ± 1
	1.	120 ± 0		91 ± 1		73 ± 1		60 ± 1		50 ± 1	
50	0.	97 ± 0	108 ± 0	74 ± 0	82 ± 1	59 ± 1	65 ± 1	49 ± 1	53 ± 1	41 ± 1	44 ± 1
	.25	98 ± 0	108 ± 0	75 ± 0	82 ± 1	59 ± 1	65 ± 1	49 ± 1	53 ± 1	41 ± 1	44 ± 1
	.5	98 ± 0	107 ± 0	75 ± 0	81 ± 1	60 ± 1	64 ± 1	49 ± 1	53 ± 1	41 ± 1	44 ± 1
	.75	99 ± 0	106 ± 0	76 ± 0	81 ± 1	60 ± 1	64 ± 1	50 ± 1	52 ± 1	42 ± 1	44 ± 1
	1.	103 ± 0		78 ± 0		62 ± 1		51 ± 1		43 ± 1	

TABLE 3

NODAL SHIFT DUE TO GRAVITOMAGNETIC PRECESSION: $a = 1$

R_p	$e \rightarrow$	0.		.2		.4		.6		.8	
↓	$\mu_- \downarrow$	+	−	+	−	+	−	+	−	+	−
	0.	8538 ± 0	...	6548^{+432}_{-427}	...	5322^{+598}_{-584}	...	4498^{+657}_{-632}	...	3909^{+669}_{-635}	...
	.25	8623 ± 0	...	6609^{+454}_{-450}	...	5370^{+626}_{-613}	...	4537^{+685}_{-662}	...	3943^{+694}_{-663}	...
5	.5	8882 ± 0	...	6799^{+532}_{-530}	...	5520^{+722}_{-714}	...	4662^{+781}_{-765}	...	4050^{+783}_{-759}	...
	.75	9341 ± 0	...	7151 ± 723	...	5808 ± 955	...	4907^{+1008}_{-1005}	...	4265^{+991}_{-987}	...
	1.	...		8143^{+1701}_{-1792}		6732^{+2184}_{-2193}		5752^{+2208}_{-2196}		5035 ± 2075	
	0.	3066 ± 0	4132 ± 0	2366 ± 81	3216 ± 480	1914^{+113}_{-110}	2622 ± 586	1601^{+125}_{-120}	2204^{+574}_{-582}	1373^{+127}_{-121}	1897^{+526}_{-546}
	.25	3089 ± 0	4121 ± 0	2382 ± 84	3204^{+469}_{-467}	1926^{+117}_{-114}	2611 ± 573	1611^{+129}_{-123}	2194^{+561}_{-570}	1381^{+131}_{-124}	1888^{+515}_{-535}
10	.5	3161 ± 0	4084 ± 0	2434 ± 93	3168 ± 434	1966^{+128}_{-126}	2576^{+531}_{-533}	1642^{+140}_{-136}	2163^{+523}_{-533}	1407^{+141}_{-136}	1859^{+481}_{-501}
	.75	3300 ± 0	4005 ± 0	2535 ± 115	3094 ± 370	2044 ± 155	2508^{+457}_{-460}	1706^{+166}_{-164}	2101^{+453}_{-464}	1460^{+165}_{-162}	1804^{+420}_{-439}
	1.	3695 ± 0		2834 ± 213		2284^{+273}_{-276}		1905^{+280}_{-285}		1630^{+268}_{-276}	
	0.	1708 ± 0	2276 ± 0	1317 ± 31	1741 ± 130	1062 ± 43	1396^{+161}_{-165}	884^{+48}_{-46}	1157^{+160}_{-167}	754^{+49}_{-46}	983^{+149}_{-159}
	.25	1718 ± 0	2269 ± 0	1325 ± 32	1736 ± 128	1068 ± 44	1391^{+158}_{-162}	889^{+49}_{-47}	1153^{+157}_{-164}	758^{+50}_{-47}	980^{+147}_{-156}
15	.5	1752 ± 0	2245 ± 0	1349 ± 35	1716 ± 120	1086 ± 48	1375^{+149}_{-153}	903 ± 52	1139^{+149}_{-155}	770^{+53}_{-51}	968^{+139}_{-148}
	.75	1818 ± 0	2195 ± 0	1396 ± 41	1677 ± 105	1122 ± 56	1343^{+132}_{-135}	932 ± 60	1112^{+133}_{-138}	793 ± 60	945^{+125}_{-132}
	1.	2018 ± 0		1542 ± 67		1235 ± 87		1023 ± 91		869^{+88}_{-90}	
	0.	1129 ± 0	1476 ± 0	870 ± 16	1123 ± 54	700 ± 22	895^{+67}_{-69}	581 ± 24	738^{+68}_{-71}	494^{+25}_{-23}	623^{+64}_{-68}
	.25	1135 ± 0	1471 ± 0	874 ± 16	1119 ± 53	703 ± 22	892^{+66}_{-68}	584 ± 25	735^{+67}_{-70}	496 ± 25	621^{+63}_{-67}
20	.5	1154 ± 0	1455 ± 0	888 ± 17	1107 ± 50	714 ± 24	883^{+63}_{-65}	592 ± 26	727^{+64}_{-67}	503 ± 26	615^{+60}_{-64}
	.75	1193 ± 0	1423 ± 0	915 ± 20	1083 ± 45	734 ± 27	864 ± 57	608 ± 29	712^{+58}_{-60}	516^{+33}_{-29}	602^{+55}_{-58}
	1.	1312 ± 0		1001 ± 30		800 ± 40		660 ± 42		559 ± 41	
	0.	818 ± 0	1051 ± 0	630 ± 9	798 ± 28	506 ± 13	634 ± 35	420 ± 14	521 ± 36	356 ± 14	439^{+34}_{-36}
	.25	822 ± 0	1048 ± 0	633 ± 9	796 ± 27	508 ± 13	632 ± 35	421 ± 14	520^{+35}_{-37}	358 ± 15	438^{+33}_{-35}
25	.5	835 ± 0	1037 ± 0	642 ± 10	787 ± 26	515 ± 14	626 ± 33	427 ± 15	515 ± 34	362 ± 15	434^{+32}_{-34}
	.75	860 ± 0	1014 ± 0	660 ± 11	771 ± 23	529 ± 16	613 ± 30	437 ± 17	504 ± 31	370 ± 17	425^{+29}_{-31}
	1.	939 ± 0		716 ± 17		572 ± 22		471 ± 23		398 ± 22	
	0.	629 ± 0	796 ± 0	484 ± 6	603 ± 16	388 ± 8	479 ± 21	322 ± 9	393 ± 21	273 ± 9	330 ± 20
	.25	632 ± 0	793 ± 0	486 ± 6	602 ± 16	390 ± 9	477 ± 20	323 ± 9	392 ± 21	273 ± 9	329 ± 20
30	.5	641 ± 0	785 ± 0	492 ± 6	596 ± 15	395 ± 9	473 ± 20	326 ± 10	388 ± 20	276 ± 10	327 ± 19
	.75	659 ± 0	769 ± 0	505 ± 7	584 ± 14	404 ± 10	464 ± 18	334 ± 11	381 ± 19	282 ± 11	321 ± 18
	1.	715 ± 0		545 ± 10		434 ± 14		357 ± 14		302 ± 15	
	0.	503 ± 0	628 ± 0	387 ± 4	476 ± 10	310 ± 6	378 ± 13	257 ± 6	309 ± 14	217 ± 6	260 ± 13
	.25	505 ± 0	627 ± 0	389 ± 4	475 ± 10	312 ± 6	377 ± 13	258 ± 6	309 ± 14	218 ± 7	259 ± 13
35	.5	512 ± 0	620 ± 0	393 ± 4	470 ± 10	315 ± 6	373 ± 13	260 ± 7	306 ± 13	220 ± 7	257 ± 13
	.75	525 ± 0	608 ± 0	403 ± 5	462 ± 9	322 ± 7	366 ± 12	266 ± 7	301 ± 12	225 ± 7	253 ± 12
	1.	567 ± 0		432 ± 7		344 ± 9		283 ± 10		239 ± 10	
	0.	415 ± 0	512 ± 0	319 ± 3	388 ± 7	256 ± 4	307 ± 9	211 ± 5	252 ± 9	179 ± 5	211 ± 9
	.25	416 ± 0	511 ± 0	320 ± 3	387 ± 7	256 ± 4	307 ± 9	212 ± 5	251 ± 9	179 ± 5	211 ± 9
40	.5	422 ± 0	506 ± 0	324 ± 3	383 ± 7	259 ± 4	304 ± 9	214 ± 5	249 ± 9	181 ± 5	209 ± 9
	.75	432 ± 0	496 ± 0	331 ± 4	377 ± 6	264 ± 5	299 ± 8	218 ± 5	245 ± 8	184 ± 5	206 ± 8
	1.	464 ± 0		354 ± 5		282 ± 6		232 ± 7		195 ± 7	
	0.	350 ± 0	428 ± 0	269 ± 2	324 ± 5	215 ± 3	256 ± 7	178 ± 4	210 ± 7	150 ± 4	176 ± 7
	.25	351 ± 0	426 ± 0	270 ± 2	323 ± 5	216 ± 3	256 ± 7	178 ± 4	209 ± 7	151 ± 4	176 ± 7
45	.5	355 ± 0	422 ± 0	272 ± 2	320 ± 5	218 ± 3	254 ± 6	180 ± 4	208 ± 7	152 ± 4	174 ± 6
	.75	363 ± 0	415 ± 0	278 ± 3	315 ± 5	222 ± 4	250 ± 6	183 ± 4	204 ± 6	155 ± 4	172 ± 6
	1.	389 ± 0		297 ± 4		236 ± 5		194 ± 5		163 ± 5	
	0.	300 ± 0	364 ± 0	230 ± 2	275 ± 4	185 ± 2	218 ± 5	152 ± 3	178 ± 5	129 ± 3	150 ± 5
	.25	301 ± 0	363 ± 0	231 ± 2	275 ± 4	185 ± 3	218 ± 5	153 ± 3	178 ± 5	129 ± 3	149 ± 5
50	.5	305 ± 0	360 ± 0	234 ± 2	272 ± 4	187 ± 3	216 ± 5	154 ± 3	177 ± 5	130 ± 3	148 ± 5
	.75	311 ± 0	353 ± 0	238 ± 2	268 ± 3	190 ± 3	212 ± 4	157 ± 3	174 ± 5	132 ± 3	146 ± 5
	1.	332 ± 0		253 ± 3		201 ± 4		165 ± 4		139 ± 4	

REFERENCES

Abramowicz, M. A. 1987, in Proc. 11th Int. Conf. on General Relativity and Gravitation, ed. M. A. H. MacCallum (Cambridge: Cambridge Univ. Press), 1
———. 1992, in Proc. Second Maryland Astrophys. Conf., Testing the AGN Paradigm, ed. S. S. Holt, S. G. Neff, & C. M. Urry (New York: AIP), 69
Abramowicz, M. A., Bao, G., Fiore, F., Lanza, A., Massaro, E., Perola, G. C., Spiegel, E. A., & Szuszkiewicz, E. 1992, in Physics of Active Galactic Nuclei, ed. W. J. Duschl & S. J. Wagner (Heidelberg: Springer)
Abramowicz, M. A., Bao, G., Karas, V., & Lanza, A. 1993, A&A, 272, 400
Abramowicz, M. A., Bao, G., Lanza, A., & Zhang, X.-H. 1989, in Proc. 23d ESLAB Symp. on Two Topics in X-Ray Astronomy, ed. J. Hunt & B. Battrick (ESA SP-296), 871
———. 1991, A&A, 245, 454
Asaoka, I. 1989, PASJ, 41, 763
Bao, G. 1992a, A&A, 257, 594
———. 1992b, Ph.D. thesis (Trieste: Int. School for Advanced Studies)
Bardeen, J. M. 1973, in Black Holes, ed. C. DeWitt & B. S. DeWitt (New York: Gordon & Breach), 215
Bardeen, J. M., & Petterson, J. A. 1975, ApJ, 195, L65
Baring, M. G. 1992, Nature, 360, 109
Begelman, M. C., Blandford, R. D., & Rees, M. J. 1984, Rev. Mod. Phys., 56, 255
Bičák, J., & Janiš, V. 1985, MNRS, 212, 899
Binney, J., & Tremaine, S. D. 1987, Galactic Dynamics (Princeton: Princeton Univ. Press)
Blandford, R. D., Netzer, H., & Woltjer, L. 1990, in Active Galactic Nuclei, ed. T. J.-L. Curvoisier & M. Mayor (Berlin: Springer-Verlag)
Blandford, R. D., & Znajek, R. L. 1977, MNRAS, 179, 433
Boyle, C. B., & Walker, I. W. 1986, MNRAS, 222, 559
Braginskij, V. B., Polnarev, A. G., & Thorne, K. S. 1984, Phys. Rev. Lett., 53, 863
Byrd, P. F., & Friedman, M. D. 1971, Handbook of Elliptic Integrals for Engineers and Scientists (Berlin: Springer-Verlag)
Carter, B. 1968, Phys. Rev., 174, 1559
Carter, B., & Luminet, J.-P. 1983, A&A, 121, 97
Chagelishvili, G. D., Lominadze, J. G., & Rogava, A. D. 1989, ApJ, 347, 1100
Chandrasekhar, S. 1983, The Mathematical Theory of Black Holes (Oxford: Clarendon)
Ciufolini, I. 1986, Phys. Rev. Lett., 56, 278
Cunningham, C. T. 1975, ApJ, 202, 788
———. 1976, ApJ, 208, 534
Cunningham, C. T., & Bardeen, J. M. 1973, ApJ, 183, 237
Damour, T., & Taylor, J. H. 1992, Phys. Rev. D, 45, 1840
de Felice, F., Nobili, L., & Calvani, M. 1974, A&A, 30, 111
Done, C., Koyama, K., Kunieda, H., Madejski, G., Mushotzky, R., & Turner, T. J.1990, in IAU Colloq. 129, Structure and Emission Properties of Accretion Disks, ed. C. Bertout et al. (Paris: Editions Frontières), 417
Done, C., Madejski, G. M., Mushotzky, R. F., & Turner, T. J. 1992, ApJ, 400, 138
Dressler, A. 1989, in IAU Symp. 134, Active Galactic Nuclei, ed. D. E. Osterbrock & J. S. Miller (Dordrecht: Kluwer), 217
Dressler, A., & Richstone, D. O. 1988, ApJ, 324, 701
———. 1990, ApJ, 348, 120
Ernst, F. J. 1976, J. Math. Phys., 17, 54
Everitt, C. W. F. 1974, in Proc. Course 56 of the International School of Physics "Enrico Fermi," Experimental Gravitation, ed. B. Berlotti (New York: Academic), 331
Fabian, A. C., Pringle, J. E., & Rees, M. J. 1975, MNRAS, 172, 150
Falcke, H., Biermann, P. L., Duschl, W. J., & Mezger, P. G. 1993, A&A, 270, 102
Ferraz-Mello, S. 1981, AJ, 86, 619
Fióre, F., Massaro, E., & Barone, P. 1992, A&A, 261, 405
Frank, J., King, A. R., & Raine, D. J. 1985, Accretion Power in Astrophysics (Cambridge: Cambridge Univ. Press)
Frank, J., & Rees, M. J. 1976, MNRAS, 176, 633
Gradshteyn, I. S., & Ryzhik, I. W. 1980, Table of Integrals, Series, and Products (New York: Academic)
Guilbert, P. W., Fabian, A. C., & Ross, R. R. 1982, MNRAS, 199, 763
Halpern, J. P., & Filippenko, A. V. 1988, Nature, 331, 46
Hills, J. G. 1988, Nature, 331, 687
Honma, F., Matsumoto, R., Kato, S., & Abramowicz, M. A. 1991, PASJ, 43, 261
Kaburaki, O., & Okamoto, I. 1991, Phys. Rev. D, 43, 340
Karas, V. 1991, MNRAS, 249, 122
Karas, V., Vokrouhlický, D., & Polnarev, A. 1992, MNRAS, 259, 569
King, A. R., & Done, C. 1993, MNRAS, in press
Kormendy, J. 1988a, ApJ, 325, 128
———. 1988b, ApJ, 335, 40
Kumar, S., & Pringle, J. E. 1985, MNRAS, 213, 435
Lecar, M., Wheeler, J. C., & McKee, C. F. 1976, ApJ, 205, 556
Lee, H.-M., & Ostriker, J. P. 1986, ApJ, 310, 176
Lense, J., & Thirring, H. 1918, Phys. Z., 19, 156
Luminet, J.-P., & Marck, J.-A. 1985, MNRAS, 212, 1029
Macdonald, D. A., & Thorne, K. S. 1982, MNRAS, 198, 345
Manko, V. S., & Sibgatullin, N. R. 1992, Phys. Rev. D, 46, 4122
Mittaz, J. P. D., & Branduardi-Raymont, G. 1989, MNRAS, 238, 1029
Moskalik, P., & Sikora, M. 1986, Nature, 319, 649
Mushotzky, R. F. 1982, ApJ, 256, 92
Novikov, I. D., Pethick, C. J., & Polnarev, A. G. 1992, MNRAS, 255, 276
Okamoto, I., & Kaburaki, O. 1991, MNRAS, 250, 300
Ostriker, J. P. 1983, ApJ, 273, 99
Park, S. J., & Vishniac, E. T. 1989, ApJ, 337, 78
Peters, P. C., & Mathews, J. 1963, Phys. Rev., 131, 435
Phinney, E. S. 1983, Ph.D. thesis, Cambridge Univ.
Press, W. H., & Teukolsky, S. A. 1977, ApJ, 213, 183
Press, W. H., Wiita, P. J., & Smarr, L. L. 1975, ApJ, 202, L135
Rees, M. J. 1988, Nature, 333, 523
———. 1993, in The Renaissance of General Relativity and Cosmology: A Survey Meeting to Celebrate the 65th Birthday of Dennis Sciama, ed. G. F. R. Ellis, A. Lanza, & J. C. Miller (Cambridge: Cambridge Univ. Press)
Rees, M. J., Ruffini, R., & Wheeler, J. A. 1974, Black Holes, Gravitational Waves and Cosmology (New York: Gordon & Breach)
Sargent, W. L., Young, P. J., Boksenberg, A., Shortridge, K., Lynds, C. R., & Hartwick, F. D. A. 1978, ApJ, 221, 731
Shlosman, I., Begelman, M. C., & Frank, J. 1990, Nature, 345, 679
Sikora, M., & Begelman, M. C. 1992, Nature, 356, 224
Stewart, J., & Walker, M. 1973, in Springer Tracts in Modern Physics, Vol. 69, Black Holes: The Outside Story, ed. G. Höhler (Berlin: Springer-Verlag)
Stoghianidis, E., & Tsoubelis, D. 1987, Gen. Relativ. Grav., 19, 1235
Syer, D., Clarke, C. J., & Rees, M. J. 1991, MNRAS, 250, 505
Tassoul, J.-L. 1988, ApJ, 324, L71
Vio, R., Turolla, R., Cristiani, S., & Barbieri, C. 1993, ApJ, 405, 163
Vokrouhlický, D., & Karas, V. 1993, MNRAS, 265, 365
Wallinder, F. H. 1991, MNRAS, 253, 184
———. 1992, NORDITA preprint
Wilkins, D. C. 1972, Phys. Rev. D, 5, 814
Will, C. M. 1993, Theory and Experiment in Gravitational Physics (Cambridge: Cambridge Univ. Press)
Young, P. J., Westphal, J. A., Kristian, J., & Wilson, C. P. 1978, ApJ, 221, 721
Zahn, J.-P. 1977, A&A, 57, 394
———. 1989, A&A, 220, 112
Zahn, J.-P., & Bouchet, L. 1989, A&A, 223, 112
Zel'dovich, Ya. B., & Novikov, I. D. 1971, Stars and Relativity (Chicago: Univ. Chicago Press)
Zentsoya, A. S. 1983, Ap&SS, 95, 11
———. 1985, Astron. Zh., 62, 1227
Zurek, W. H., Siemiginowska, A., & Colgate, S. A. 1992, in Proc. Second Maryland Astrophysical Conf., Testing the AGN Paradigm, ed. S. S. Holt, S. G. Neff, & C. M. Urry (New York: AIP), 564